

## METHODS OF PHYSICAL EXPERIMENT

# Test Experiments on Muon Radiography with Emulsion Track Detectors in Russia

**A. B. Aleksandrov<sup>a</sup>, A. V. Bagulya<sup>a</sup>, M. M. Chernyavsky<sup>a</sup>, V. I. Galkin<sup>b, c</sup>, L. G. Dedenko<sup>b, c</sup>,  
N. V. Fomenko<sup>a</sup>, N. S. Konovalova<sup>a</sup>, G. De Lellis<sup>f</sup>, A. K. Managadze<sup>b</sup>, O. I. Orurk<sup>d</sup>,  
N. G. Polukhina<sup>a</sup>, T. M. Roganova<sup>b</sup>, T. V. Shchedrina<sup>a</sup>, C. Sirignano<sup>g</sup>, N. I. Starkov<sup>a</sup>,  
Tan Naing So<sup>a</sup>, V. E. Tioukov<sup>a</sup>, M. S. Vladimirov<sup>a</sup>, and S. G. Zemskova<sup>a, e</sup>**

<sup>a</sup>*Lebedev Physical Institute, Russian Academy of Sciences, Moscow, 119991 Russia*

<sup>b</sup>*Skobeltsyn Institute of Nuclear Physics, Moscow State University, Moscow, 119991 Russia*

<sup>c</sup>*Faculty of Physics, Moscow State University, Moscow, 119991 Russia*

<sup>d</sup>*Research Institute of Tire Industry, Moscow, 105118 Russia*

<sup>e</sup>*Joint Institute for Nuclear Research, Dubna, Moscow oblast, 141980 Russia*

<sup>g</sup>*Istituto Nazionale di Fisica Nucleare – Sezione di Napoli – Complesso Universitario di M.S. Angelo,  
Ed. 6 - Via Cintia, Napoli, 80126 Italy*

<sup>f</sup>*Istituto Nazionale di Fisica Nucleare Sezione di Padova, Padova, 35131 Italy  
e-mail: poluhina@sci.lebedev.ru*

**Abstract**—In Russia, the Lebedev Physical Institute of the Russian Academy of Sciences and the Skobeltsyn Institute of Nuclear Physics of Moscow State University are starting a series of pilot muon radiography experiments with nuclear emulsion detectors to study the interior structure of large-scale natural and industrial objects. As a result, the optimal conditions for experimental organization have been determined, algorithms of data processing have been worked out, and peculiarities of the method have been ultimately investigated. Here we present the experimental data, including field observations (in the mine of Geophysical department of Russian Academy of Sciences) confirming the availability of the method with track detectors on the base of nuclear emulsions with uniquely high spatial resolution, providing their high-tech automated processing.

**DOI:** 10.1134/S1547477115050027

## INTRODUCTION

Muon radiography is a method of investigating the structures of massive natural and industrial objects lying in the registration of muons flux level after passing through the substance of the studied object. The muons fluxes of cosmic rays at the Earth's surface are used as a translucent beam. Both electronic and emulsion particle detectors can be used as recorders. This paper presents the first results on the application of researching objects by muon radiography with track detectors based on nuclear photoemulsion. These detectors are autonomous, modular, and easily relocatable devices.

Muon radiography is used as a promising addition to geophysical and geological methods [1] when analyzing the seismic and karst processes [2], for mineral exploration, for the radiation monitoring of a nuclear power plants complex [3], and for the implementation of the nondestructive testing of industrial facilities (blast furnaces, bridge supports, etc.) [4]. This method makes it possible to explore underground caves and large cavities of artificial origin. It is used to monitor the state of long-term underground storage, which

requires detailed knowledge of the geological environment (the composition and boundaries of different layers), for monitoring in the mining industry, and for many other applications.

The method is based on using muons fluxes of cosmic origin, which make up about 80% of all observed particles of secondary cosmic radiation at sea level. Muons originate as a result of decay of charged  $\pi$  and  $K$  mesons, which are formed in the upper atmosphere during the interaction of nuclear-active particles of primary cosmic radiation with the atom nuclei in the Earth's atmosphere. The lifetime of  $t_0$  muons is about  $2.197 \times 10^{-6}$  s, but the cosmic ray muons at speed  $v$  are close to the speed of light, live significantly longer in accordance with the ratio

$$t = \frac{t_0}{\sqrt{1 - \left(\frac{v}{c}\right)^2}},$$

and can propagate over long distances.

Muons are not nuclear-active particles and lose their energy mainly due to electromagnetic interac-

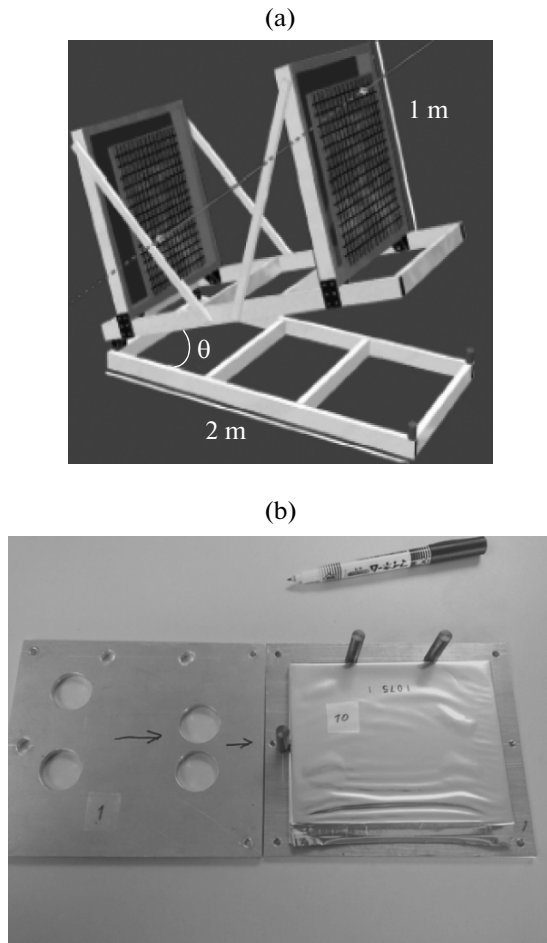


**Fig. 1.** Comparison of sizes of (Fig. 1a) electronic [6] and (Fig. 1b) emulsion track detectors for muon radiography (Fig. 1b, on the right, six layers of emulsion lie on metal plate packed in metallized package; Fig. 1b, on the left the upper metal plate for fixation of emulsions is shown). Emulsion panel with a thickness of 0.5 cm with several layers of emulsions (Fig. 1b) exceeds in the angular resolution the electronic telescope with base of  $\geq 1$  m shown in Fig. 1a.

tions with the electrons and nuclei of matter. The lack of strong interactions and relatively large rest mass of muons determine their high penetration ability compared to hadrons, electrons, and  $\gamma$  quanta. As a result, the muons of the cosmic ray not only overcome the Earth's atmosphere, but also penetrate deep into the soil, depending on their energy. Muons with energies of  $E_\mu \sim 10^{12} - 10^{13}$  eV reaching the sea level are recorded in underground experiments at depths of up to 8.6 km of water equivalent. The flux of penetrating muons at sea level is about 104 particles/(m<sup>2</sup> min).

The distribution features of atmospheric muons allow their use in muon radiography to study the structure of major natural and artificial objects. The change of distribution of substance density within an object is done by recording muons coming from the object by detectors of charged elementary particles (e.g., nuclear emulsion). Comparing the muon density flux

$\Phi$  after passing through the target with a flux free falling from the atmosphere  $\Phi_0$ , one can define the opacity  $\zeta$  of investigated dense structures and their individual regions. The spectrum of atmospheric muons is continuous, and the flux of muons emerging from the studied object is the integral flux on energy varying from the minimum initial energy  $E_{min}(\zeta)$  needed to cross the thick medium on the thickness of L up to the maximum value:

$$\Phi = \int_{E_{min}(\zeta)}^{\infty} \Phi(E) dE.$$

The final number of registered muons depends on the intensity of the muon flux, crossing the target, exposure time, and sensitivity and area of the detector and can be evaluated based on the model calculations with taking into account the conditions of the experiment. Analysis of angular distributions of muons after their passing through the object located above the monitoring level allows one to make a conclusion about the distribution of density of the substance, including the existence of heterogeneities in its depth.

The direction of each muon in the detector is determined by the values of the azimuthal and zenithal angles ( $\varphi$ ,  $\theta$ ) with respect to an axis perpendicular to the plane of the detector, the sizes which are significantly smaller than the sizes of the studied object. Muons forming an image of the object satisfy the following condition: the distance from the point of the muon entering the object up to the point in which its energy becomes zero must be greater than the length of the path of muon in the object. The number of muons passing through an object depends on the direction of their arrival (values of  $\theta$  and  $\varphi$ ) and the density of the medium substance  $\rho(\theta, \varphi)$ . Modeling the muon flux passing through the object and comparing simulation results with experimental data allow one to reconstruct the features of the internal structure of the object.

#### ADVANTAGES OF USING OF EMULSION TRACK DETECTORS IN THE MUON RADIOGRAPHY

Until recently in the international practice of conducting research with the use of muon radiography, electronic equipment was mainly used [5, 6]; this is much more cumbersome and complex to operate than track detectors based on nuclear emulsions, which many experimental groups have started actively using recently (Fig. 1). The main advantages of emulsion track detectors, in addition to their small sizes and design simplicity, are their good spatial ( $< 1 \mu\text{m}$ ) and angular ( $\sim 1 \text{ msr}$ ) resolution, large information capacity, ease of transport, and ease of operation in difficult conditions (for example, in area of volcanoes). The most important advantages of nuclear emulsions are

their independence from supply sources and the lack of need for an electronic reader system during exposure.

The size and, respectively, weight of the emulsion detector track may be relatively small while maintaining the necessary efficiency due to high coordinate resolution of emulsions. An emulsion panel of 0.5 cm thickness with several layers of nuclear emulsions will exceed upon angular resolution an electronic telescope with base  $\sim 1 \text{ m}^2$ , like the one shown in Fig. 1a. However, this does not mean that the emulsion detector must have a significantly smaller area than an electronic one, because the volume of collected statistics depends on the value of detector area. Detector size (area and number of layers of photoemulsion) is determined by the desired sensitivity, depending on the expected angular and linear sizes of studied object.

Experiments carried out by the muon radiography method using emulsion track detectors are successfully implemented in a number of research centers owing to the development of automated methods of processing of emulsion data [6, 7]. Experiments of this kind in Russia, until recently, have not been carried out due to a lack of reliable manufacturer of nuclear emulsions. However, in recent years the production of nuclear emulsions with characteristics needed for the registration of relativistic particles has been organized at OAO Slavich, Pereslavl-Zalessky, Yaroslavl oblast, Russia, which allowed employees of the Lebedev Physical Institute of the Russian Academy of Sciences and Skobeltsyn Institute of Nuclear Physics of Moscow State University to carry out the first test experiments on the application of the method.

### TEST EXPERIMENTS USING MUON RADIOGRAPHY

In 2012–2014, the employees of the Lebedev Physical Institute of the Russian Academy of Sciences and Skobeltsyn Institute of Nuclear Physics of Moscow State University have carried out a number of test experiments to introduce a muon radiography method in which the relativistic nuclear emulsions were used as muons detectors. The object of the first test experiment on muon radiography was a steel column weighing 23 t (cyclotron magnet yoke of the Skobeltsyn Institute of Nuclear Physics of Moscow State University), which played the role of a massive absorber of atmospheric muons and created a “shadow” in the flux of these particles (Fig. 2).

In the experiment, nuclear emulsion produced by the Russian company OAO Slavich and the Japanese company Fuji Photo Film were used, which were used in the OPERA international experiment [8]. The detectors prepared for the tests consisted of densely packed stacks of emulsion plates with sizes of  $10 \times 12 \text{ cm}^2$  rigidly fastened in frames of aluminum plates. Details of the construction of detectors are shown in Figs. 1b and 2a.

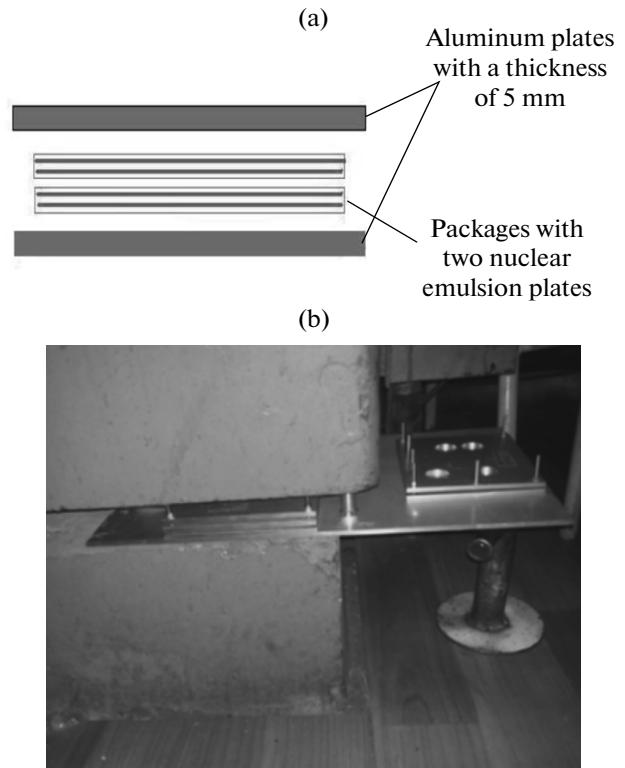


**Fig. 2.** Assembling the emulsion detectors for the first experiment on muon radiography in the Lebedev Physical Institute of the Russian Academy of Sciences and the Skobeltsyn Institute of Nuclear Physics of Moscow State University: (a) the arrangement of emulsion layers between the metal plates and (b) the photo of muon radiography detectors installed in the body of steel columns of the absorber and outside it.

The detectors installed in the body of steel columns and the outside column according to Fig. 2b were exposed for 49 days.

The processing of emulsion data was carried out by employees of Lebedev Physical Institute of the Russian Academy of Sciences and Skobeltsyn Institute of Nuclear Physics of Moscow State University having at their disposal complexes of measuring instruments equipped by optical tables with high-precision displacement and high-resolution digital video cameras for recording and digitizing optical images. PAVICOM (Lebedev Physical Institute of the Russian Academy of Sciences) and VISKAN-500 (Skobeltsyn Institute of Nuclear Physics of Moscow State University) automated measuring complexes, designed to meet the necessary requirements, enables us to accomplish the high-speed scanning of nuclear emulsions and process the images in real time.

The result of scanning of each emulsion plate is a data array that specifies with high accuracy the trajectory of each particle registered by detector, including zenithal and azimuthal angles of incidence, used in this methodology. The data obtained during automatic

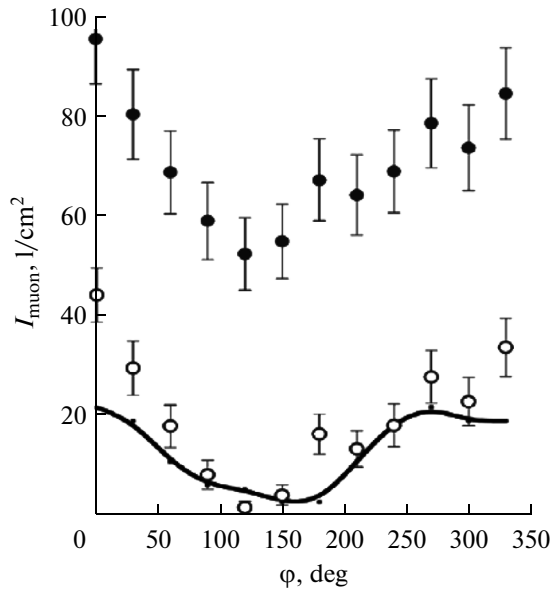
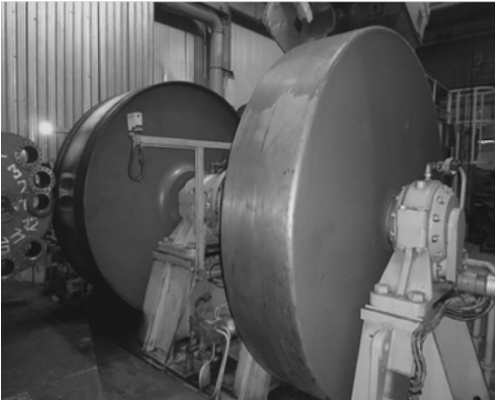


**Fig. 3.** Angular distributions of muon fluxes at different azimuthal angles  $\varphi$  and a fixed range of zenithal angles  $\theta$  obtained as a result of the first test experiment in comparison with the results of the model calculations: — calculation, ● experiment, ○ experiment with subtraction of background for 2 months.

(a)



(b)

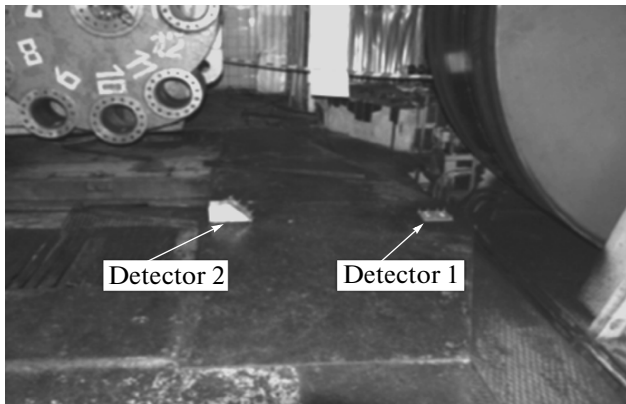


**Fig. 4.** (a) Test stand, the massive parts of which (3 m in diameter each) are recorded by the muon radiography method; (b) location of detectors on the test stand.

analysis are subjected to background subtraction. It consists of recording instrumental effects, falsely reconstructed tracks, effects related to the transportation of the detector, etc.

Angular distributions of particles obtained in the first test experiment demonstrated changes in muon fluxes entering the detector in a selected angle range, depending on the length of the path in the iron absorber (column). The distributions are in full accordance with the predictions of the model calculations (Fig. 3).

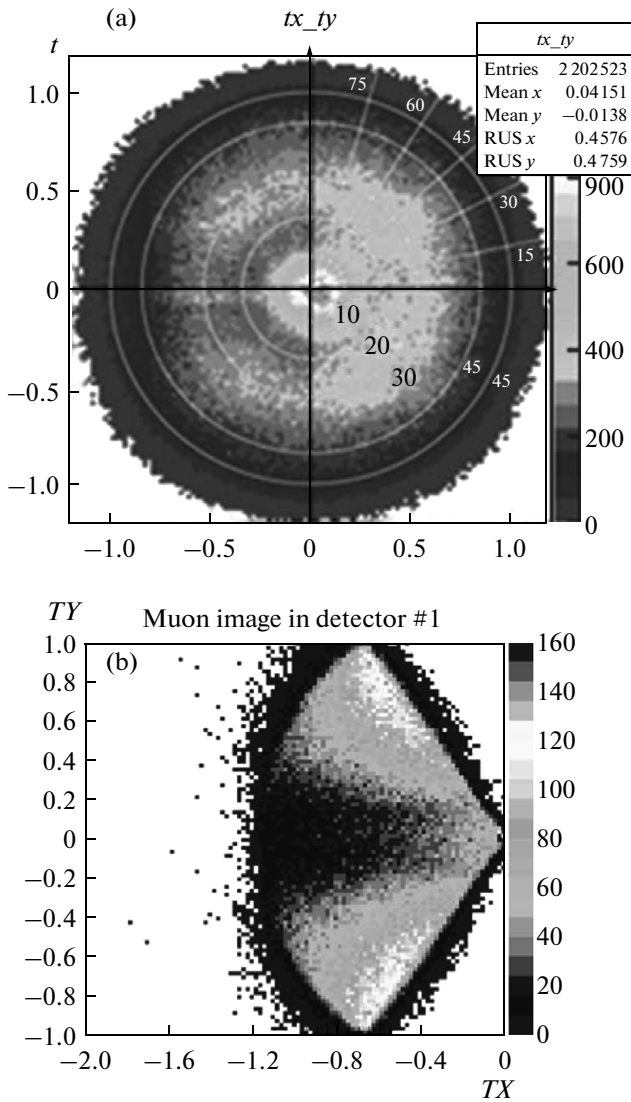
The second test experiment was carried out on the territory of OOO NITs NIISHP, Moscow, Russia, from June 13 to October 25, 2013; i.e., the exposure of detectors was 135 days. The object under observation was disks of the running drum that is the inertial element of a test stand weighing 40 t (Fig. 4). The assembly scheme of emulsion track detectors was similar to the previous experiment; only in this case each detector included three packages with two layers of emulsions instead of two packages, like in the first experiment.

Figure 5 presents the experimental angular distribution of muons (Fig. 5a) and corresponding model calculations (Fig. 5b) for detector 1. The “shadow” from the running drum of test stand is clearly visible on both graphs. The experimental data are in a good agreement with the calculation results.

To present the results,  $tx$  and  $ty$  variables were chosen that are the tangents of tilt angles of tracks in projections on a plane  $xz$ ,  $yz$  where  $tx = \frac{dx}{dz} = \tan(\theta)\cos(\phi)$  and  $ty =$

$\frac{dy}{dz} = \tan(\theta)\sin(\phi)$  in the coordinates of the emulsion film. For readability, the coordinate grid ( $\theta$ ,  $\varphi$ ) ( $\theta$  is the circles and  $\varphi$  is the rays coming from the origin) was superimposed on the plane of  $tx$ – $ty$  of Fig. 5a in accordance with ratios of  $\tan(\varphi) = ty/tx$  and  $\tan^2(\theta) = tx^2 + ty^2$ .

The third experiment on the muon radiography method was carried out at a depth of 30 m in the underground shaft located in the territory of the Geophysical Survey of the Russian Academy of Sciences (Obninsk, Moscow oblast, Russia). As a result of the experiment, it was intended to record the difference of atmospheric muons fluxes on the Earth’s surface and at depth in the shaft after passing the soil layer. For that, the detectors were installed on two levels (Figs. 6, 7). Among the objectives of the experiment, it was also the estimation of the possibility to detect the cavities (lift shaft) in the thickness of the soil using the detector with nuclear photoemulsion located at a depth of 30 m. When  $\theta \sim 25^\circ$  and  $\varphi \sim 135^\circ$ , i.e., in the direction of the lift shaft (Figs. 6, 7), the absorption of muons was weakened due to the presence of cavity, and hence the muon flux from this direction must noticeably to exceed the background.



**Fig. 5.** Angular distributions of muons in detector 1 after the passing of the substance of test stand: (a) experimental distributions obtained in the nuclear emulsion of detector 1; (b) results of the model calculations.

In order to determine the optimal exposure time sufficient to obtain the necessary information, the detectors were exposed during different periods on time (2 and 4 months).

The implemented model calculations confirm that the signal from the lift shaft must noticeably become apparent in the muon flux entering the detector. Figure 8 presents a calculated graph of distribution of muon fluxes as a function of the angles  $\theta$  and  $\varphi$  in the direction of the lift shaft.

Figures 9a and 9b show the obtained experimental distribution of muons that passed through detector 6, being exposed at a depth of 30 m in 4 months.

To select the tracks from exposure during the experiment from the rest of the background tracks, an

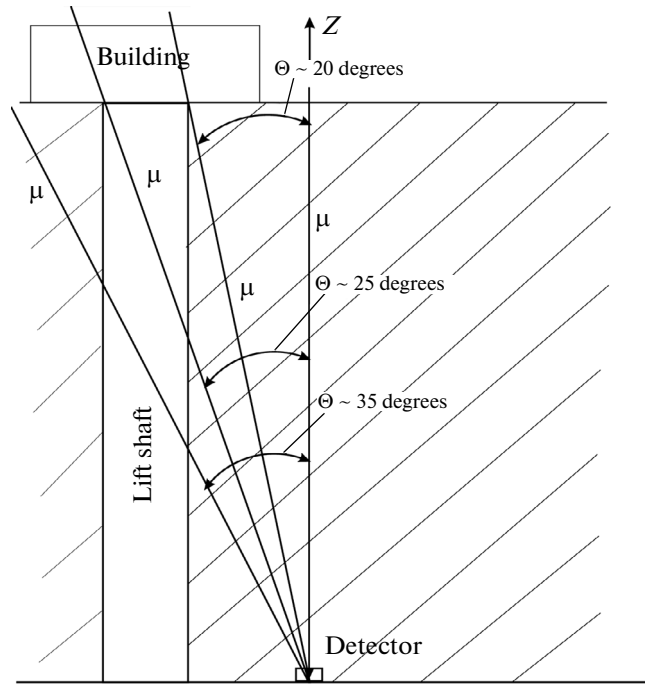


**Fig. 6.** Outline of experiment in the shaft at a depth of 30 m: (a) the lateral image of lift shaft and underground detectors. The range of the angle  $\theta$  ( $20^\circ$ – $35^\circ$ ) in which the signal from the shaft should be observed is shown; (b) relative location of the lift shaft and underground detectors (top view). The orientation of the  $x$  and  $y$  axes in the detector system is shown.

average by azimuthal angle background ( $\varphi$ ) was subtracted from the original distribution ( $tx$ ,  $ty$ ). This method gives a more vivid picture of the density difference of tracks. Figure 9a presents the results. At this distribution, the signal from the lift shaft is clearly visible (marked by a white frame). In addition, other heterogeneities in soil are clearly visible on the histogram. Figure 9b shows the distribution by the angle  $\varphi$  in the coordinate system of the emulsion films. Also, the clear peak in the direction of the location of the lift shaft  $\varphi \sim 135^\circ$  is seen on this distribution. The presence of other features of distribution by  $\varphi$  is associated with heterogeneities of soil composition in the area of the shaft. There are large muon fluxes in the direction area across of the shaft corridor located in the marble-like limestone lens.

Muon fluxes in the surface and underground detectors at a depth of 30 m differ about fifty times, which is in good agreement with the calculated estimates.

Figure 10 presents the result of a more detailed analysis of the results of the 4-month exposure underground of detector 6 in Obninsk. The comparison of the value of muon flux exceeding the background in the area of shaft by the angle of  $\varphi \sim 135^\circ$  and in several sectors by the angle  $\theta$  (I for  $0^\circ$ – $10^\circ$ ; II for  $10^\circ$ – $20^\circ$ ; III for  $20^\circ$ – $30^\circ$ ; IV for  $30^\circ$ – $40^\circ$ ; and V for  $40^\circ$ – $50^\circ$ ). As expected, in sectors I and II, the signal from the shaft

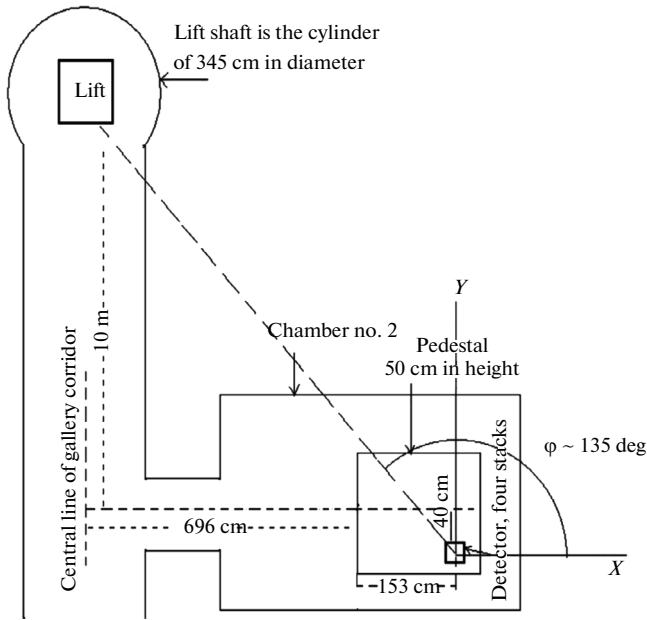


**Fig. 7.** Relative location of the lift shaft and underground detectors (top view). The orientation of the  $x$  and  $y$  axes in the detector and the direction to the lift shaft are shown.

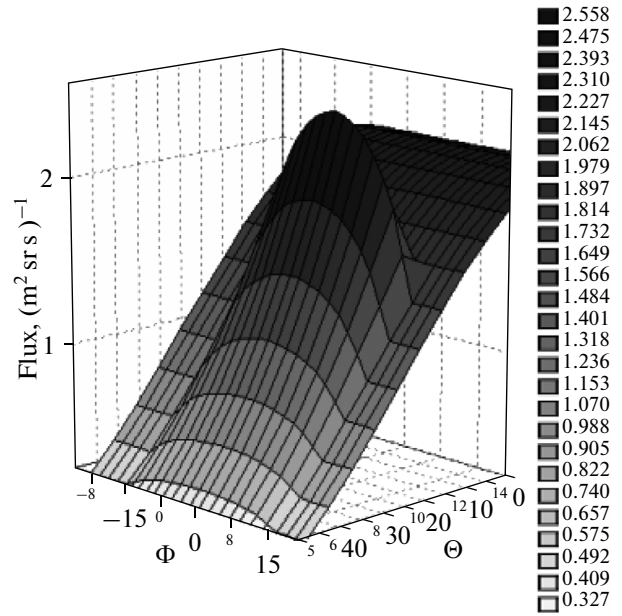


**Fig. 8.** 3D-image of the angular dependence of the muon fluxes at the point of detectors location underground.

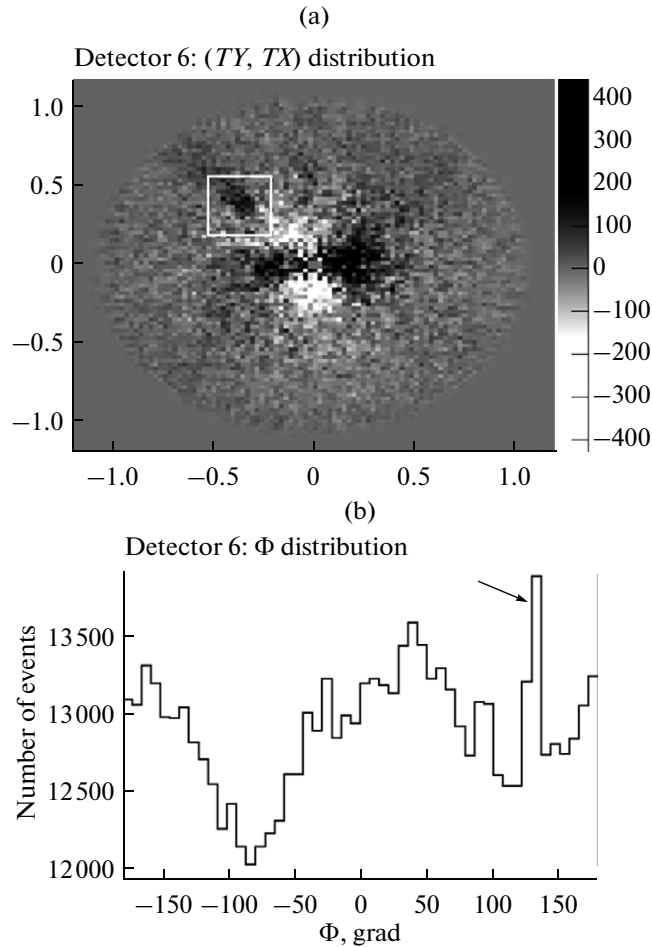


**Fig. 9.** (a) 2D-distribution  $(tx, ty)$  of muon flux at a depth of 30 m after subtracting of background, average by angle  $\varphi$ ; (b) distribution of muon flux at a depth of 30 m on the azimuthal angle  $\varphi$ ; peak in the area of  $135^\circ$  corresponds to the lift shaft.

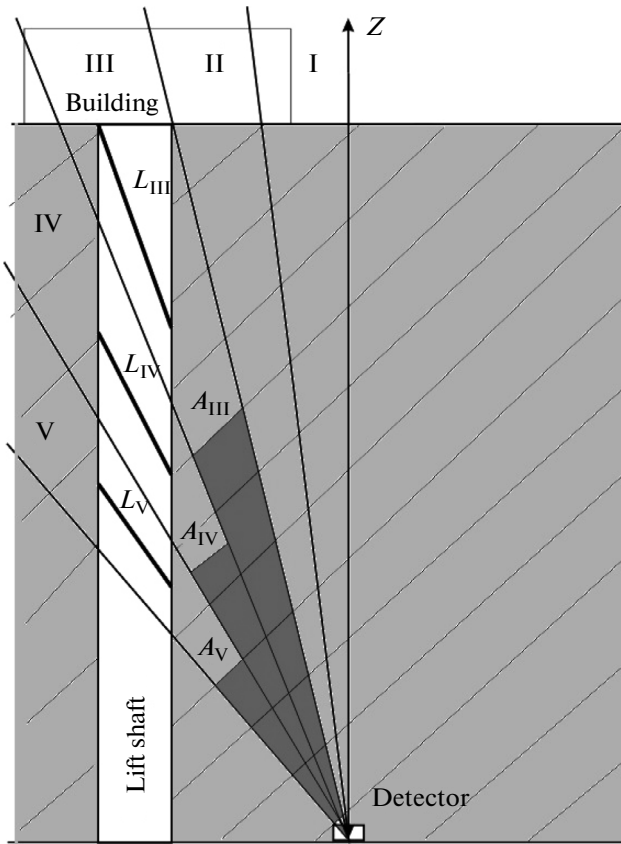


**Fig. 10.** Comparison of the value of muon flux exceeding the background in the area of shaft by the angle of  $\varphi \sim 135^\circ$  and in several sectors by the angle  $\theta$ . Roman numerals designate the ranges of angles  $\theta$ : I for 0–10, II for 10–20, III for 20–30, IV for 30–40, and V for 40–50. Bold lines  $L_i$  are marked the segments of path of muons in a shaft in different ranges of  $\theta$  ( $L_I = L_{II} = 0$ ). Darkened zones of sectors are proportional to the excess of muon flux over the background (amplitude of signal is  $A_i$ ) in different ranges. The lengths of line segments are equal to  $L_{III} = 8.3$  m,  $L_{IV} = 6.1$  m, and  $L_V = 4.9$  m. Excess of fluxes (in the arbitrary units) is as follows:  $A_{III} = 1700$ ;  $A_{IV} = 1340$ ;  $A_V = 830$ . The ratio of the lengths of the line segments is as follows:  $L_{III} : L_{IV} = 1.36$ ;  $L_{IV} : L_V = 1.53$ . The ratio of the quantities of measured fluxes is as follows:  $A_{III} : A_{IV} = 1.26$ ;  $A_{IV} : A_V = 1.41$ .

is missing. The correlation of fluxes in sectors III, IV, and V approximately corresponds to the ratios of lengths of the line segments passed by muons inside the shaft in the same sectors. It should not be in overall agreement, because the relationship between paths passed in the soil by particle and residual flux is non-linear.

## CONCLUSIONS

An analysis of the results obtained in test experiments by employees of Lebedev Physical Institute of the Russian Academy of Sciences and the Skobel'syn Institute of Nuclear Physics of Moscow State Univer-

sity by muon radiography indicates that, in accordance with the predictions of the model calculations, the emulsion track technique allows us to obtain reliable data on the features of structure of investigated objects. Spatial distributions of muon fluxes measured in test experiments and a calculated prediction of heterogeneities in the structure of objects in general give a good agreement. This is evidence of the possibility of development of muon radiography in Russia using the emulsion track detectors of the proposed design and processing facilities of emulsion data that Russian institutes have available.

## REFERENCES

1. J. Marteau, D. Gibert, N. Lesparre, F. Nicollin, P. Noli, and F. Giacoppo, "Muons tomography applied to geosciences and volcanology," *Nucl. Instrum. Methods Phys. Res. A* **695** 23–28 (2012).
2. H. K. M. Tanaka, H. Miyajima, T. Kusagaya, A. Taketa, T. Uchida, and M. Tanaka, "Cosmic muon imaging of hidden seismic fault zones: rainwater permeation into the mechanical fractured zones in Itoigawa-Shizuoka tectonic line, Japan," *Earth Planet. Sci. Lett.* **306**, 156–162 (2011).
3. C. L. Morris, C. C. Alexander, J. D. Bacon, K. N. Borozdin, D. J. Clark, R. Chartrand, C. J. Espinoza, A. M. Fraser, M. C. Galassi, J. A. Green, J. S. Gonzales, J. J. Gomez, N. W. Hengartner, G. E. Hogan, A. V. Klimenko, et al., "Tomographic imaging with cosmic ray muons," *Sci. Global Secur.* **16**, 37–53 (2008).
4. W. B. Gilboy, P. M. Jenneson, S. J. R. Simons, S. J. Stanley, and D. Rhodes, "Muon radiography of large industrial structures," *Nucl. Instrum. Methods Phys. Res. B* **263**, 317–319 (2007).
5. N. Lesparre, J. Marteau, Y. Declais, D. Gibert, B. Carlus, F. Nicollin, and B. Kergosien, "Design and operation of a field telescope for cosmic ray geophysical tomography," *Geosci. Instrum. Method. Data Syst.* **1**, 33–42 (2012).
6. C. Carloganu, V. Niess, S. Bene, E. Busato, P. Dupieux, F. Fehr, P. Gay, D. Miallier, B. Vulpesu, P. Boivin, C. Combaret, P. Labazuy, I. Laktineh, J.-F. Lenat, L. Mirabito, and A. Portal, "Towards a muon radiography of the puy de dome," *Geosci. Instrum. Method. Data Syst.* **2**, 55–60 (2013).
7. H. K. M. Tanaka, "Evaluation of positioning and density profiling accuracy of muon radiography by utilizing a 15-ton steel block," *Geosci. Instrum. Method Data Syst.* **2**, 79–83 (2013).
8. N. Yu. Agafonova, A. B. Aleksandrov, A. M. Anokhina, A. V. Bagulya, M. S. Vladimirov, Yu. A. Gornushkin, T. A. Dzhatdov, S. G. Dmitrievskii, R. I. Enikeev, S. G. Zemskova, D. K. Levashev, A. S. Mal'gin, V. A. Matveev, D. V. Naumov, V. V. Nikitina, et al., "Search for the  $\nu_\mu \rightarrow \nu_\tau$  neutrino oscillation with the OPERA hybrid detector," *Phys. Part. Nucl.* **44**, 657–703 (2013).

Translated by M. Kromin